UC Davis

UC Davis Previously Published Works

Title

Kv2.1 channels play opposing roles in regulating membrane potential, Ca^{2+} channel function, and myogenic tone in arterial smooth muscle.

Permalink

https://escholarship.org/uc/item/07s8q2k5

Journal

Proceedings of the National Academy of Sciences of the United States of America, 117(7)

ISSN

0027-8424

Authors

O'Dwyer, Samantha C
Palacio, Stephanie
Matsumoto, Collin
et al.

Publication Date

2020-02-01

DOI

10.1073/pnas.1917879117

Peer reviewed

eScholarship.org Powered by the California Digital Library
University of California

Kv2.1 channels play opposing roles in regulating membrane potential, Ca^{2+} channel function, and myogenic tone in arterial smooth muscle

Samantha C. O'Dwyer[a], Stephanie Palacio[a], Collin Matsumoto[a], Laura Guarina[a], Nicholas R. Klug[a,1], Sendoa Tajada[a], Barbara Rosati[a,b], David McKinnon[a,b], James S. Trimmer[a], and L. Fernando Santana[a,2]

[a]Department of Physiology and Membrane Biology, School of Medicine, University of California, Davis, CA 95616; and [b]Department of Physiology and Biophysics, Renaissance School of Medicine, Stony Brook University, The State University of New York, Stony Brook, NY 11794

Edited by Mark T. Nelson, University of Vermont, Burlington, VT, and approved January 9, 2020 (received for review October 11, 2019)

The accepted role of the protein Kv2.1 in arterial smooth muscle cells is to form K^+ channels in the sarcolemma. Opening of Kv2.1 channels causes membrane hyperpolarization, which decreases the activity of L-type $Ca_V1.2$ channels, lowering intracellular Ca^{2+} ($[Ca^{2+}]_i$) and causing smooth muscle relaxation. A limitation of this model is that it is based exclusively on data from male arterial myocytes. Here, we used a combination of electrophysiology as well as imaging approaches to investigate the role of Kv2.1 channels in male and female arterial myocytes. We confirmed that Kv2.1 plays a canonical conductive role but found it also has a structural role in arterial myocytes to enhance clustering of $Ca_V1.2$ channels. Less than 1% of Kv2.1 channels are conductive and induce membrane hyperpolarization. Paradoxically, by enhancing the structural clustering and probability of $Ca_V1.2$–$Ca_V1.2$ interactions within these clusters, Kv2.1 increases Ca^{2+} influx. These functional impacts of Kv2.1 depend on its level of expression, which varies with sex. In female myocytes, where expression of Kv2.1 protein is higher than in male myocytes, Kv2.1 has conductive and structural roles. Female myocytes have larger $Ca_V1.2$ clusters, larger $[Ca^{2+}]_i$, and larger myogenic tone than male myocytes. In contrast, in male myocytes, Kv2.1 channels regulate membrane potential but not $Ca_V1.2$ channel clustering. We propose a model in which Kv2.1 function varies with sex: in males, Kv2.1 channels control membrane potential but, in female myocytes, Kv2.1 plays dual electrical and $Ca_V1.2$ clustering roles. This contributes to sex-specific regulation of excitability, $[Ca^{2+}]_i$, and myogenic tone in arterial myocytes.

voltage-gated calcium channels | voltage-gated potassium channels | calcium channel clustering

The smooth muscle cells lining the walls of small resistance arteries and arterioles contract in response to increases in intravascular pressure (1). Due to its important role in regulating blood pressure, the molecular and biophysical mechanisms underlying this myogenic response have been the subject of intense investigation for decades. This work has led to the formulation of a model in which the myogenic response is initiated when membrane stretch activates Na^+-permeable canonical TRPC6, melastatin-type TRPM4, and TRPP1 (PKD2) channels (2–4). The opening of these channels depolarizes arterial smooth muscle cells, thereby activating voltage-gated, dihydropyridine-sensitive L-type $Ca_V1.2$ Ca^{2+} channels. Ca^{2+} influx through $Ca_V1.2$ channels causes a local elevation in intracellular free Ca^{2+} ($[Ca^{2+}]_i$) called a "$Ca_V1.2$ sparklet" (5–7). The simultaneous activation of multiple $Ca_V1.2$ sparklets produces a global increase in $[Ca^{2+}]_i$ that triggers contraction.

A salient property of $Ca_V1.2$ channels is their intrinsic ability to form clusters via a stochastic self-assembly mechanism (8). Channels within these clusters undergo functional coupling in response to local elevations in $[Ca^{2+}]_i$ (9–11). Coupled gating of clustered $Ca_V1.2$ channels is dynamic and involves cytoplasmic C tail–C tail interactions initiated by Ca^{2+} binding to calmodulin (11, 12). The consequence of $Ca_V1.2$ channel coupling is that it allows more Ca^{2+} influx than random openings of independently gating channels. Coupled gating of $Ca_V1.2$ channels accounts for ~50% of Ca^{2+} influx in arterial smooth muscle (7). At present, however, the mechanisms controlling clustering of $Ca_V1.2$ channels are unknown.

Negative feedback regulation of Ca^{2+} influx via $Ca_V1.2$ channels occurs through the activation of voltage-dependent Kv2.1 and Kv1.5 K^+ channels as well as large-conductance, Ca^{2+}-activated K^+ (BK) channels (13–15). In cerebral arterial myocytes, Kv2.1 associates with "silent" Kv9.3 subunits in heteromeric complexes. This association has important physiological consequences, as it results in hyperpolarizing shifts in the voltage-dependent activation of Kv2.1 currents, making Kv2.1/Kv9.3 channel currents the predominant K^+ conductance determining membrane potential over the lower physiological range of intravascular pressures (40 to 80 mmHg) (16). Acute pharmacological blockade or knockdown of Kv2.1 eliminates a substantial component of delayed rectifier current in arterial myocytes, suggesting that Kv2.1 channels are activated by membrane depolarization and conduct K^+ in these

Significance

Our data challenge the generally accepted view that Kv2.1 proteins regulate arterial smooth muscle function by regulating their membrane potential. Rather, we discovered that Kv2.1 plays both conductive and structural roles with opposing functional consequences on arterial myocytes, with the former predominating in males, the latter in females. Opening of Kv2.1 channels opposes vasoconstriction by inducing membrane hyperpolarization. In addition to this conductive function, Kv2.1 promotes the structural clustering of $Ca_V1.2$ channels, thereby enhancing Ca^{2+} influx and inducing vasoconstriction. These two functions are highlighted by differences in the regulation of membrane potential, intracellular Ca^{2+}, and myogenic tone between males and females. Our data suggest that these disparities derive from sex-specific variations in Kv2.1 expression levels in male versus female myocytes.

Author contributions: S.C.O., J.S.T., and L.F.S. designed research; S.C.O., S.P., C.M., L.G., N.R.K., and S.T. performed research; B.R., D.M., and J.S.T. contributed new reagents/analytic tools; S.C.O., S.P., C.M., L.G., N.R.K., and S.T. analyzed data; and S.C.O., J.S.T., and L.F.S. wrote the paper.

Competing interest statement: L.F.S. and M.T.N. are both affiliated with the University of Vermont.

This article is a PNAS Direct Submission.

This open access article is distributed under Creative Commons Attribution-NonCommercial-NoDerivatives License 4.0 (CC BY-NC-ND).

[1]Present address: Department of Pharmacology, University of Vermont, Burlington, VT 05405.

[2]To whom correspondence may be addressed. Email: lfsantana@ucdavis.edu.

This article contains supporting information online at https://www.pnas.org/lookup/suppl/doi:10.1073/pnas.1917879117/-/DCSupplemental.

First published February 3, 2020.

cells (14, 16–19). Accordingly, acute inhibition of Kv2.1 with stromatoxin 1 (ScTx1) caused constriction in rat cerebral artery smooth muscle (14).

Intriguingly, almost all plasma membrane Kv2.1 channels are nonconductive in heterologous cells (20–22). If also true for native cells, it would raise an important but difficult question: What is the function of these nonconductive Kv2.1 channels? Recent studies suggest a potential answer to this question. Like $Ca_V1.2$ channels, Kv2.1 channels are expressed in clusters in the surface membrane of neurons and mammalian heterologous expression systems (23–29). Importantly, Vierra et al. (30) recently showed that clustered Kv2.1 colocalizes with $Ca_V1.2$ channels and that coexpression with Kv2.1 translates into an increase in the cluster size and activity of coexpressed $Ca_V1.2$ channels in both HEK-293 cells and hippocampal neurons. In smooth muscle cells, $Ca_V1.2$ clustering is critical for functional coupling and the development of myogenic tone (6, 7). It is currently unknown whether Kv2.1 channels have similar roles in smooth muscle to regulate $Ca_V1.2$ channel clustering and hence function.

Here, we tested the hypothesis that Kv2.1 channels have dual conducting and structural roles in arterial smooth muscle. Our data challenge the conventional view that Kv2.1 has solely a conductive role in arterial myocytes. Rather, our data support our hypothesis that in arterial myocytes, Kv2.1 plays both conductive and structural roles with opposing functional consequences. Conductive Kv2.1 channels oppose vasoconstriction by inducing membrane hyperpolarization. Paradoxically, by promoting the structural clustering of the $Ca_V1.2$ channel, Kv2.1 enhances Ca^{2+} influx and induces vasoconstriction. We found that Kv2.1 protein is expressed to a larger extent in female than in male arterial smooth muscle. Sex-specific disparities in Kv2.1 expression shift the balance between the membrane hyperpolarization and Ca^{2+} entry actions of Kv2.1, leading to differences in the regulation of membrane potential, $[Ca^{2+}]_i$, and myogenic tone between males and female arterial myocytes.

Results

Sexual Dimorphism in the Expression of Kv2.1 Channels in Arterial Smooth Muscle. We began our study by recording voltage-gated K^+ (I_K) currents elicited in response to 500-ms depolarizations to voltages ranging from −50 to +50 mV in male and female mesenteric artery smooth muscle cells (*SI Appendix*, Fig. S1). In these cells, I_K currents are produced by the opening of Kv and BK channels. To quantify the contribution of Kv (I_{Kv}) and BK (I_{BK}) currents to I_K, K^+ currents were recorded before and after the application of the specific BK channel blocker iberiotoxin (IBTX; 100 nM). Accordingly, we identified I_{BK} as the IBTX-sensitive component of composite K^+ currents. IBTX-insensitive currents are produced by Kv channels (i.e., I_{Kv}). *SI Appendix*, Fig. S1*A* shows I_K, I_{Kv}, and I_{BK} currents from representative wild-type (WT) female and male mesenteric myocytes. Note that I_K tended to be larger in female than in male myocytes (*SI Appendix*, Fig. S1*B*). This was due to larger I_{Kv} (*SI Appendix*, Fig. S1*C*), but not I_{BK}, in female myocytes (*SI Appendix*, Fig. S1*D*).

We sought to determine whether these differences in I_{Kv} were associated with variations in Kv2.1 channel activity. To do this, we recorded I_K in male and female WT and Kv2.1-null ($Kv2.1^{-/-}$) myocytes before and after the application of the Kv2.1 blocker ScTx1 (100 nM) (14) in the sustained presence of IBTX (100 nM) (Fig. 1*A*). Kv2.1 currents ($I_{Kv2.1}$) were evoked by 500-ms steps to voltages ranging from −50 to +50 mV. In concordance with the I_{Kv} data above, $I_{Kv2.1}$ were about 60% smaller in male than in female WT myocytes. ScTx1-sensitive currents were never observed in $Kv2.1^{-/-}$ myocytes (Fig. 1*B*).

Next, we determined Kv2.1 protein expression levels in male and female mesenteric arteries (Fig. 1 *C* and *D*). Immunoblots of WT arteries showed prominent bands at 110 kDa, the expected

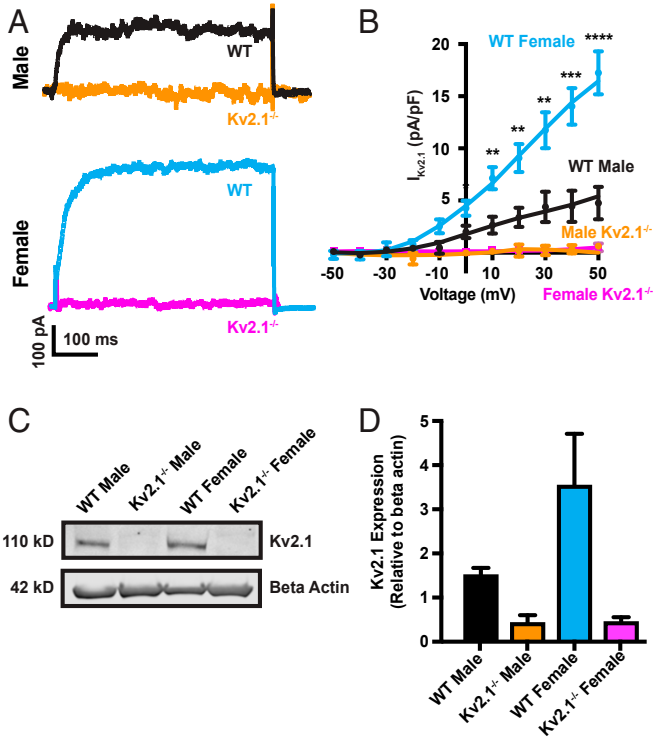

Fig. 1. Female mesenteric myocytes express more Kv2.1 protein and have larger ionic Kv2.1 currents than male myocytes. (*A*) $I_{Kv2.1}$ records (+50 mV) from representative WT and $Kv2.1^{-/-}$ male and female smooth muscle cells. $I_{Kv2.1}$ traces were obtained by subtracting the currents after the application of ScTx1 from control currents (i.e., I_K). (*B*) Current–voltage relationship of $I_{K2.1}$. (*C*) Images of immunoblots of Kv2.1 and β-actin using WT and $Kv2.1^{-/-}$ mesenteric arteries. (*D*) The bar plot shows the intensities of the Kv2.1 band in all arteries examined. $*P < 0.05$, $**P < 0.01$, $***P < 0.001$, $****P < 0.0001$. Error bars indicate mean ± SEM.

molecular mass of Kv2.1 (19, 31). This band was absent in lysates obtained from $Kv2.1^{-/-}$ arteries. Interestingly, the intensity of the Kv2.1 band in the immunoblots was 45 ± 5% higher in WT female versus male arteries, suggesting sex-specific differences in the expression of this channel protein. Consistent with the electrophysiological data (Fig. 1*A* and *SI Appendix*, Fig. S1), we found that Kv1.5, a major contributor to the ScTx1-insensitive component of I_K (15), and BK channel protein levels were similar in WT male and female arteries (*SI Appendix*, Fig. S2).

Most Kv2.1 Channels in the Sarcolemma of Male and Female Arterial Myocytes Are Nonconductive. A limitation of our immunoblot analysis is that it was performed using whole-artery homogenates and hence did not allow us to determine the level of plasma membrane Kv2.1 expression in mesenteric myocytes. To determine the number of plasma membrane Kv2.1 channels, we calculated the time integral of the ON gating charge associated with activation of Kv2.1 channels ($Q_{on,Kv2.1}$), which is proportional to the number of these voltage-gated channels in the plasma membrane. The ON gating charge is described by the equation $Q_{on,Kv2.1} = N_{Kv2.1} * q_{Kv2.1}$, where N is the number of channels and q is the number of elementary charges per channel, and is independent of the open probability (P_o) and amplitude of elementary Kv2.1 currents ($i_{Kv2.1}$). Thus, $Q_{on,Kv2.1}$ can be used to estimate the number of Kv2.1 channels in the sarcolemma of isolated mesenteric myocytes.

We recorded Q_{on} under conditions in which K^+, Ca^{2+}, Na^+, and Cl^- ionic conductances were eliminated before and after the application of the tarantula venom peptide guangxitoxin-1E

(GxTx1E; 1 μM; Fig. 2*A* and *SI Appendix*, Fig. S3), which binds to and immobilizes the voltage sensors of Kv2.1 channels (32). Consequently, $Q_{on,Kv2.1}$ was defined as the GxTx1E-sensitive component of Q_{on} in arterial myocytes. As shown in Fig. 2 *A* and *B* and consistent with the immunoblot data above, the amplitude of $Q_{on,Kv2.1}$ was larger (~50%) in female than in male arterial myocytes. Two observations indicate that the $Q_{on,Kv2.1}$ we recorded were indeed the result of voltage-induced movement of charged particles in the S4 segment of sarcolemmal Kv2.1 channels and not produced by other voltage-gated channels (e.g., $Ca_V1.2$, Kv1.5) or membrane capacitance. First, we did not detect GxTx1E-sensitive gating currents in Kv2.1$^{-/-}$ myocytes. Second, the voltage dependence of $Q_{on,Kv2.1}$ was sigmoidal and not linear as would be expected if it were produced solely by charging the plasma membrane (Fig. 2*C*). The voltage at which half of the normalized $Q_{on,Kv2.1}$ was detected ($V_{1/2}$) was similar in male ($V_{1/2}$ = −3 ± 2 mV) and female ($V_{1/2}$ = −2 ± 1 mV) myocytes. While our $Q_{on,Kv2.1}$ $V_{1/2}$ values are more depolarized than the values of ~−25 mV reported in previous studies of gating currents in heterologous cells with exogenous expression of Kv2.1 (21, 33–36), we note that a recent study (32) yielded a value (−10 mV) more similar to that obtained here. All of these previous studies were performed on cells expressing homomeric recombinant Kv2.1 channels, and our study records gating currents from endogenous Kv2.1 channels. Arterial myocytes are known to express Kv9.3 electrically silent subunits (16, 37, 38), and while gating currents from heteromeric Kv2.1/Kv9.3 channels have not been reported, they could be distinct from those that arise from homomeric Kv2.1 channels.

For comparison, we determined the voltage dependencies of the normalized conductance (G/G_{max}) using the $I_{Kv2.1}$ data in Fig. 1*A* and superimposed it on the $Q_{on,Kv2.1}/Q_{max}$ data (Fig. 2*C*). The $V_{1/2}$ of G/G_{max} was similar in male ($V_{1/2}$ = 20 ± 2 mV) and female ($V_{1/2}$ = 18 ± 3 mV) myocytes. As expected (39), the $Q_{on,Kv2.1}$ relationship is shifted toward more negative potentials than the voltage dependence of G/G_{max} in male and female myocytes.

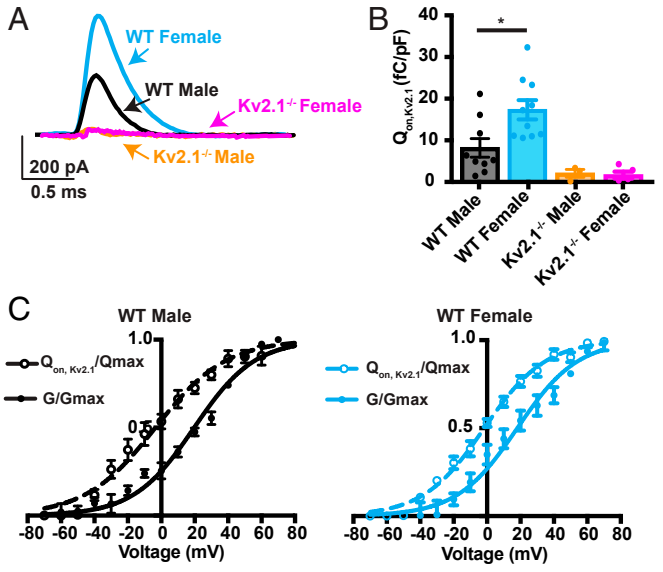

Fig. 2. Most Kv2.1 channels in the sarcolemma of male and female arterial myocytes are nonconductive. (*A*) Kv2.1 gating currents (GxTx1E-sensitive) from representative WT and Kv2.1$^{-/-}$ male and female mesenteric smooth muscle cells. (*B*) Bar plot of the total charge associated with $Q_{on,Kv2.1}$ gating currents. (*C*) Plots of the voltage dependencies of $Q_{on,Kv2.1}/Q_{max}$ (dashed lines) and Kv2.1 G/G_{max} (solid lines) in WT male (*Left*) and female (*Right*) myocytes. *P < 0.05. Error bars indicate mean ± SEM.

Next, we determined the total number of sarcolemma Kv2.1 channels in female and male myocytes. The number of Kv2.1 channels equals the total Kv2.1 charge movement per cell divided by the charge movement per channel. According to Islas and Sigworth (40), a total of 12.5 gating charges (q_e) move per Kv2.1 channel gating cycle. Thus, the total amount of charge movement per channel is 12.5 * 1.6×10^{-19} C (i.e., 2×10^{-18} C). Therefore, using our maximal $Q_{on,Kv2.1}$, we calculated that the total number of Kv2.1 channels was 183,000 ± 27,716 in female myocytes versus 75,000 ± 21,628 in male myocytes (P < 0.05), assuming that the charge movement in native myocyte Kv2.1/Kv9.3 channels is similar to that previously determined for homomeric Kv2.1 (39).

The number of conducting channels could be calculated using the equation I = N * i * P_o, where N is the number of conducting channels, i is the amplitude of elementary currents, P_o is the open probability, and I is the amplitude of the macroscopic current. For heteromeric Kv2.1/Kv9.3 channels, the $i_{Kv2.1}$ at +60 mV is 1.8 pA (37). To our knowledge, the maximum P_o of Kv2.1/Kv9.3 heteromeric channels has not been reported. However, because differences in the amplitude of macroscopic Kv2.1 and Kv2.1/Kv9.3 currents at voltages where the maximum P_o has been reached (e.g., +60 mV) seem to be exclusively due to differences in the amplitude of elementary currents only (e.g., Kv9.3 expression does not increase Kv2.1 expression) (16, 37), it is reasonable to assume that the maximum P_os of Kv2.1 and Kv2.1/Kv9.3 channels are likely similar. Accordingly, we used the maximum P_o value (i.e., 0.7) reported by Islas and Sigworth (40).

Assuming that the maximum P_o and amplitude of elementary current of Kv2.1 channels in male and female WT myocytes are similar, and using our $I_{Kv2.1}$ values, the number of conducting Kv2.1 channels was 194 ($N_{Kv2.1,female}$ = 244 pA/[1.8 pA * 0.7]) and 62 ($N_{Kv2.1,male}$ = 79 pA/[1.8 pA * 0.7]) in female and male myocytes, respectively. The percentage of functional Kv2.1-containing channels is therefore about 0.1% in both male and female myocytes. Thus, as is the case in heterologous expression systems (20–22), the vast majority of Kv2.1 channels in the sarcolemma of arterial myocytes are nonconductive.

Kv2.1 Channels Differentially Regulate the Membrane Potential, $[Ca^{2+}]_i$, and Myogenic Tone of Male and Female Arterial Myocytes. A key question raised by the electrophysiological data above is whether such a small fraction of conducting Kv2.1 channels (i.e., ~0.1%) have a functional impact on pressurized male and female mesenteric artery smooth muscle (Fig. 3). Because the generally accepted role of Kv2.1 channels is to mediate K^+ flux and hence regulate membrane excitability, we began by recording membrane potential, V_m, from pressurized, denuded WT and Kv2.1$^{-/-}$ mesenteric artery segments using sharp electrodes (Fig. 3*A*). At the physiological intravascular pressure of 80 mmHg, the smooth muscle cells of WT female arteries were more depolarized (V_m = −28 ± 2 mV) than those in male arteries (V_m = −40 ± 2 mV) (Fig. 3*B*). This was unexpected, as female myocytes express a larger number of conducting Kv2.1 channels than male myocytes.

Notably, chronic loss of Kv2.1 expression and function had different effects on the membrane potential of male and female smooth muscle (Fig. 3*B*). Consistent with their generally accepted role of opposing membrane depolarization, the membrane potential of male Kv2.1$^{-/-}$ artery smooth muscle was more depolarized (V_m = −33 ± 2 mV) than that of their WT counterparts (V_m = −40 ± 2 mV). In contrast, female Kv2.1$^{-/-}$ arteries were more hyperpolarized (V_m = −33 ± 2 mV) than WT female artery smooth muscle (V_m = −28 ± 2 mV). As such, the differences between the V_m of WT male and female myocytes were eliminated in myocytes lacking Kv2.1 expression.

We also investigated the acute effects of blocking Kv2.1 channels on smooth muscle membrane potential (Fig. 3*C*). Application of ScTx1 (100 nM) depolarized male and female

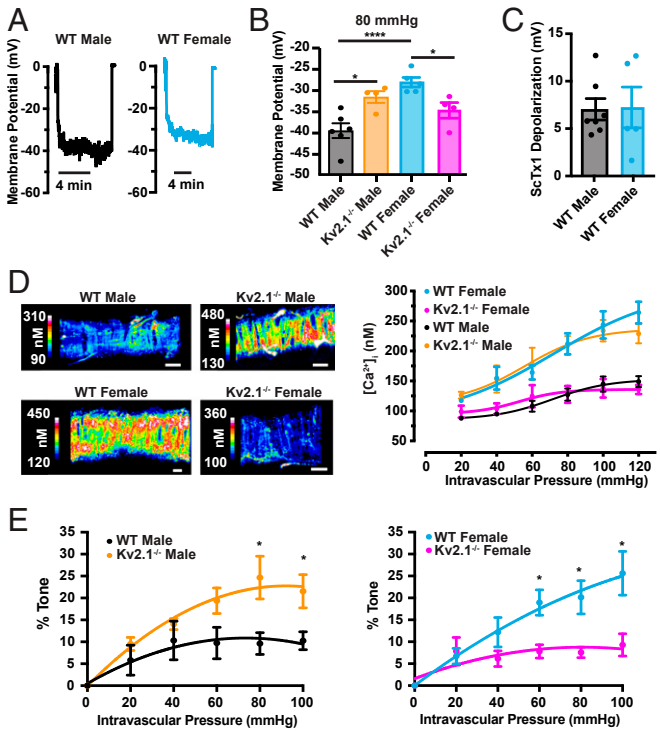

Fig. 3. Differential effects of acute and chronic loss of Kv2.1 channel function in male and female arteries. (*A*) Sharp-electrode records of the membrane potential of smooth muscle in pressurized (80-mmHg) WT female and male arteries. (*B*) Bar plot of the mean ± SEM membrane potential in WT and Kv2.1$^{-/-}$ male and female arteries. (*C*) Bar plot of the ScTx1-induced depolarization on male and female pressurized (80 mmHg) arteries. (*D*) Two-dimensional $[Ca^{2+}]_i$ images from representative pressurized (80-mmHg) WT and Kv2.1$^{-/-}$ female and male arteries. (Scale bars, 25 μm.) (*D*, *Right*) Bar plot showing $[Ca^{2+}]_i$ in WT and Kv2.1$^{-/-}$ female and male arteries at intravascular pressures ranging from 20 to 120 mmHg. (*E*) Pressure–tone relationships of WT and Kv2.1$^{-/-}$ female and male arteries. *P < 0.05, **P < 0.01, ***P < 0.001, ****P < 0.0001. Error bars indicate mean ± SEM.

arteries by 7 ± 2 and 7 ± 1 mV, respectively. ScTx1 had no effect on Kv2.1$^{-/-}$ arteries.

Next, we measured wall $[Ca^{2+}]_i$ (Fig. 3*D*) and myogenic tone (Fig. 3*E*) in male and female WT and Kv2.1$^{-/-}$ pressurized arteries. Our data indicate that $[Ca^{2+}]_i$ and myogenic tone are higher in female than in male arteries. Consistent with our membrane potential data, male Kv2.1$^{-/-}$ had higher $[Ca^{2+}]_i$ and myogenic tone than WT arteries. In sharp contrast, female Kv2.1$^{-/-}$ had lower $[Ca^{2+}]_i$ and myogenic tone than female WT arteries. Together, these data suggest that while acute changes in Kv2.1 function alter male and female smooth muscle excitability, chronic loss of these channels has sex-specific effects on smooth muscle function.

Expression of Kv2.1 Increases the Activity and Open Times of $Ca_V1.2$ Channels in Female but Not in Male Arterial Myocytes. The membrane potential of arterial myocytes is set by a balance of outward and inward currents. In principle, our observation that female WT myocytes are more depolarized than male WT myocytes could be the result of lower hyperpolarizing currents and/or up-regulation of an inward depolarizing current in female cells. One current we recently showed to be up-regulated by Kv2.1 channel expression in HEK-293 cells and hippocampal neurons is the L-type $Ca_V1.2$ channel current (I_{Ca}) (30), which can depolarize smooth muscle and also directly increase $[Ca^{2+}]_i$.

Thus, we recorded macroscopic ionic $Ca_V1.2$ currents (I_{Ca}s) from WT and Kv2.1$^{-/-}$ male and female arterial myocytes (Fig. 4*A*). I_{Ca} were evoked by 300-ms step depolarizations from the holding potential of −80 mV to voltages ranging from −70 to +60 mV. We found that the amplitude of I_{Ca} was larger in female than in male WT myocytes. Furthermore, loss of Kv1.2 channels was associated with a decrease in I_{Ca} amplitude in cells of both sexes, but the decrease in I_{Ca} was larger in female than in male Kv2.1$^{-/-}$ myocytes. The overall impact of eliminating Kv2.1 expression is that the differences between the I_{Ca} amplitude of WT male and female myocytes were eliminated in myocytes lacking Kv2.1 expression.

We also determined the voltage dependence of the normalized I_{Ca} conductance (G/G_{max}) (Fig. 4*B*). This analysis indicates that the I_{Ca} G/G_{max} relationship in WT female myocytes ($V_{1/2}$ = −10.2 ± 0.8 mV) was shifted toward more negative membrane potentials than in male myocytes ($V_{1/2}$ = −1.8 ± 1.1 mV). The $V_{1/2}$ of the G/G_{max} relationship of female Kv2.1$^{-/-}$ myocytes (−1.9 ± 2.0 mV) was similar to that of WT (P = 0.98) and Kv2.1$^{-/-}$ male myocytes (−5.8 ± 1.1 mV, P = 0.06) (Fig. 4*B*).

We next investigated the basis of the different I_{Ca} amplitudes of WT male and female myocytes. Immunoblot analysis showed that $Ca_V1.2$ protein expression was similar in WT and

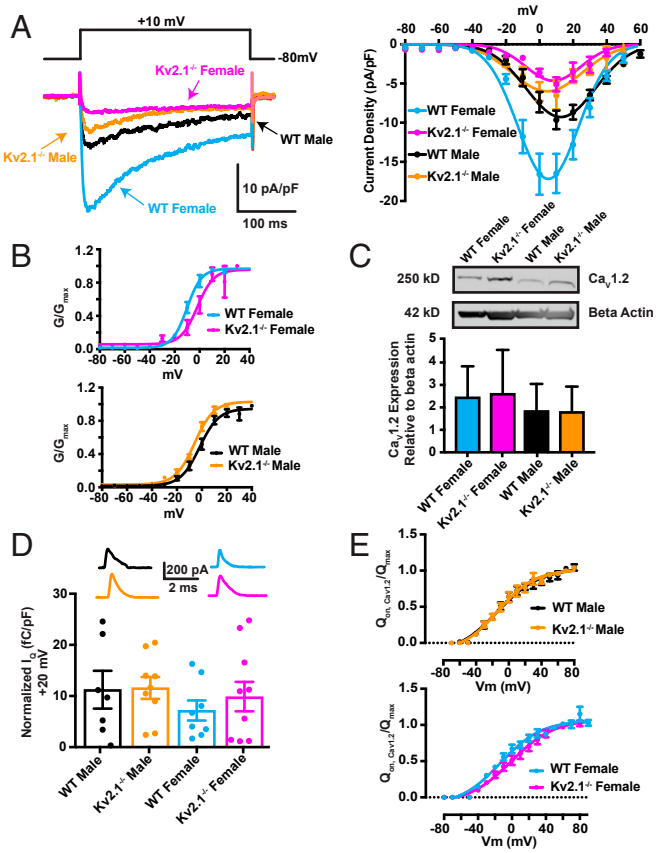

Fig. 4. Expression of Kv2.1 increases the $Ca_V1.2$ channel currents in female but not in male arterial myocytes. (*A*, *Left*) I_{Ca} records (+10 mV) from representative WT and Kv2.1$^{-/-}$ male and female myocytes. (*A*, *Right*) Voltage dependence of I_{Ca} at membrane potentials ranging from −80 to +60 mV. (*B*) Voltage dependence of the G/G_{max} of I_{Ca} in WT and Kv2.1$^{-/-}$ male and female myocytes. (*C*, *Top*) Image of a representative $Ca_V1.2$ immunoblot. (*C*, *Bottom*) Bar plot showing the $Ca_V1.2$ band intensity in WT and Kv2.1$^{-/-}$ male and female arteries. (*D*, *Top*) $Ca_V1.2$ gating current records (nitrendipine-sensitive) from representative WT and Kv2.1$^{-/-}$ female and male mesenteric smooth muscle cells. (*D*, *Bottom*) Bar plot showing the $Q_{on,Cav1.2}$ gating currents. (*E*) Plots of the voltage dependencies of $Q_{on,Cav1.2}/Q_{max}$ in WT and Kv2.1$^{-/-}$ male (*Top*) and female (*Bottom*) myocytes. Error bars indicate mean ± SEM.

Kv2.1$^{-/-}$ male and female arteries (Fig. 4*C*). As done above for Kv2.1, we followed up these experiments by recording $Ca_V1.2$ gating currents, which provide a direct measurement of the channels in the sarcolemma of arterial myocytes (Fig. 4*D*). $Ca_V1.2$ gating currents were recorded before and after the $Ca_V1.2$ voltage sensor immobilizer nitrendipine (10 μM) was applied (*SI Appendix*, Fig. S4) (41) under conditions in which ionic current was eliminated. Consistent with our immunoblot data, the maximal (at +20 mV) $Q_{on,Cav1.2}$ was similar in WT and Kv2.1$^{-/-}$ male and female myocytes ($P = 0.67$). Finally, we found that the voltage dependence of the normalized $Q_{on,Cav1.2}$ was fit with a sigmoidal function and that $V_{1/2}$ and k values were similar in WT and Kv2.1$^{-/-}$ male and female myocytes (Fig. 4 *D* and *E*).

We used $Q_{on,Cav1.2}$ data to calculate the number of $Ca_V1.2$ channels in the membrane as was done for Kv2.1 channels above. According to Noceti et al. (42), a total of 9.1 q_e gating charges move per $Ca_V1.2$ channel gating cycle. Because $Q_{on,Cav1.2}$ was similar in male and female myocytes, we combined the data into a single group. This analysis suggested that the number of $Ca_V1.2$ channels in mesenteric myocytes was 192,612 ± 19,168 channels.

Next, we recorded elementary $Ca_V1.2$ currents (i_{Ca}) (Fig. 5). $Ca_V1.2$ channel openings were evoked by 2-s step depolarizations to potentials ranging from −30 to +20 mV. Currents were recorded in cell-attached patches, with 110 mM Ba^{2+} in the pipette solution used as the charge carrier. Fig. 5*A* shows representative records of i_{Ca} from female and male WT and Kv2.1$^{-/-}$ myocytes at −30, −10, and +10 mV with the expected amplitude for this voltage and ionic conditions. The voltage dependence of unitary $Ca_V1.2$ current amplitudes is shown in Fig. 5*B*. These data were fit with a linear function that revealed that the conductance of i_{Ca} was similar in WT (female 15 + 1 pS; male 14 + 1 pS) and Kv2.1$^{-/-}$ (female 14 + 1 pS; male 16 + 1 pS) myocytes.

We determined the P_o of single $Ca_V1.2$ channels in WT and Kv2.1$^{-/-}$ female and male myocytes (Fig. 5*C*). Note that the P_o at the voltage where the peak of I_{Ca} was recorded (i.e., +10 mV; Fig. 4*A*) was largest in WT female myocytes but similar among WT male and Kv2.1$^{-/-}$ male and female cells. A consistent observation during analysis was that WT female i_{Ca} openings appeared to be longer than those in WT male and Kv2.1$^{-/-}$ male and female myocytes. Thus, we analyzed the open times of single $Ca_V1.2$ channel openings in these cells at −10 mV (*SI Appendix*, Fig. S5). Although the $Ca_V1.2$ channel open-time histogram for all cells could be fit with the sum of 2 exponential log-transformed functions with a short and long time constant of 0.7 and 20 ms, respectively, the proportion of short and long openings varied among individual myocytes. The fraction of long $Ca_V1.2$ openings was nearly 12-fold larger in WT female cells (12%) than in WT male (1%) and Kv2.1$^{-/-}$ myocytes from mice of either sex (1%).

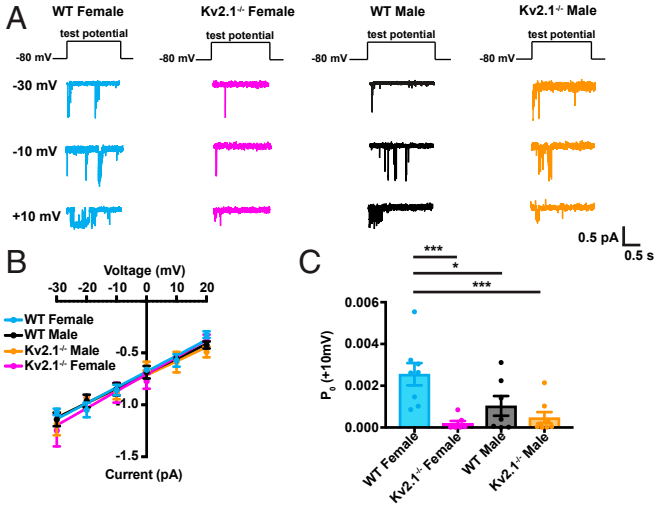

Fig. 5. $Ca_V1.2$ channels have a higher open probability and longer open times in female than in male myocytes. (*A*) Elementary $Ca_V1.2$ current records at −30, −10, and +10 mV from representative WT and Kv2.1$^{-/-}$ male and female myocytes. (*B*) Amplitude of i_{Ca} at voltages ranging from −30 to +20 mV. Solid lines are linear fits to the data. (*C*) Bar plot of the open probability (P_o) of single $Ca_V1.2$ channel currents at +10 mV in WT and Kv2.1$^{-/-}$ male and female myocytes. *$P < 0.05$, ***$P < 0.001$. Error bars indicate mean ± SEM.

Kv2.1 Channel Expression Increases $Ca_V1.2$ Channel Cluster Size in Female Myocytes to a Larger Extent than in Male Myocytes. We have previously shown that physical coupling of clustered $Ca_V1.2$ channels shifts the voltage dependence of I_{Ca} toward more negative potentials and increases the P_o and open times of $Ca_V1.2$ channels (9, 11, 12). Thus, the electrophysiological differences between male and female WT and Kv2.1$^{-/-}$ myocytes are similar to those observed with varying degrees of $Ca_V1.2$ clustering and functional $Ca_V1.2$ coupling (9, 11, 12, 43). Three previously published lines of evidence support the hypothesis that Kv2.1 regulates the spatial organization and functional state of $Ca_V1.2$ channels. First, Kv2.1 channels exist in large clusters in diverse brain neurons (23–26). A recent study indicated that Kv2.1 colocalizes with $Ca_V1.2$ channels coexpressed in heterologous HEK-293 cells (29). Finally, Vierra et al. (30) have recently shown that Kv2.1 coexpression leads to increased clustering and activity of coexpressed $Ca_V1.2$ channels in both hippocampal neurons and HEK-293 cells. Thus, we tested the hypothesis that Kv2.1 expression increases $Ca_V1.2$ clustering in arterial myocytes using ground-state depletion (GSD) superresolution imaging (Fig. 6).

SI Appendix, Fig. S6 shows representative total internal reflection fluorescence (TIRF) images of immunolabeled $Ca_V1.2$ clusters in male and female WT and Kv2.1$^{-/-}$ arterial myocytes. We found that $Ca_V1.2$-associated fluorescence intensity was similar in WT and Kv2.1$^{-/-}$ female and male myocytes, consistent with the immunoblot and gating current data (Fig. 4 *C* and *D*), leading to the conclusion that overall $Ca_V1.2$ expression does not vary among these samples. Fig. 6 illustrates representative superresolution maps of immunolabeled $Ca_V1.2$ clusters in male and female WT and Kv2.1$^{-/-}$ myocytes. Note that $Ca_V1.2$ clusters were significantly larger in female WT (4,131 ± 209.4 nm^2) than in male WT (3,492 ± 192 nm^2) myocytes. When we compared the cluster size of $Ca_V1.2$ channels in WT vs. Kv2.1$^{-/-}$ myocytes, there was a significant difference in females (WT, 4,131 ± 209 nm^2; Kv2.1$^{-/-}$, 3,395 ± 178 nm^2) but not in males (WT, 3,492 ± 192 nm^2; Kv2.1$^{-/-}$, 3,870 ± 228 nm^2); note that the sex-specific differences in cluster size observed in WT myocytes were eliminated in the Kv2.1$^{-/-}$ cells. These data are consistent with the view that, as in hippocampal neurons and HEK-293 cells (30), Kv2.1 channels promote $Ca_V1.2$ channel clustering in arterial myocytes, and that this effect is more prominent in female myocytes that express higher levels of Kv2.1.

Kv2.1 Channels Colocalize with $Ca_V1.2$ Channels and Promote $Ca_V1.2$–$Ca_V1.2$ Channel Interactions. We used a proximity ligation assay (PLA) to determine if Kv2.1 and $Ca_V1.2$ are within 50 nm of each other in arterial myocytes (Fig. 7*A*). We detected multiple puncta, indicative of $Ca_V1.2$–Kv2.1 channel proximity in male and female WT but not Kv2.1$^{-/-}$ myocytes. These observations suggest that Kv2.1 channels colocalize with $Ca_V1.2$ channels in mesenteric arterial myocytes.

Having determined that Kv2.1 and $Ca_V1.2$ channels are in close association in arterial myocytes, we investigated whether Kv2.1 promotes $Ca_V1.2$ channel–channel interactions. To test this hypothesis, we applied a bimolecular fluorescence complementation approach using $Ca_V1.2$ channels fused with either the

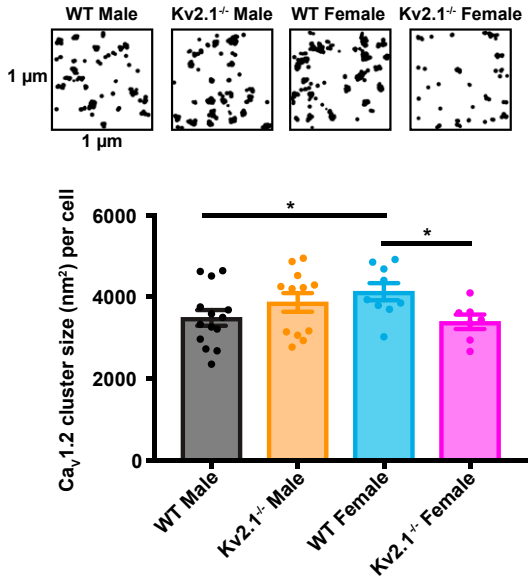

Fig. 6. Kv2.1 channel expression increases $Ca_V1.2$ channel cluster size in female myocytes to a larger extent than in male myocytes. Superresolution GSD images of regions of interest from representative Kv2.1$^{-/-}$ male and female myocytes. The bar plot shows the mean ± SEM $Ca_V1.2$ cluster area per cell. *$P < 0.05$.

N or C terminus of the split-Venus fluorescent protein system to yield $Ca_V1.2$-VN155(I152L) and $Ca_V1.2$-VC155, respectively. In isolation, VN155(I152L) and VC155 are nonfluorescent. However, when brought into close proximity by interaction of the separately tagged $Ca_V1.2$ subunits, they can reconstitute a full, fluorescent Venus protein. Thus, split-Venus fluorescence can be used to report spontaneous interactions between adjacent $Ca_V1.2$ channels (12, 44, 45). Accordingly, we compared basal split-Venus fluorescence in HEK-293 cells expressing $Ca_V1.2$-VN and $Ca_V1.2$-VC channels with or without Kv2.1. Because Venus reconstitution is virtually irreversible, once the C tails of adjacent $Ca_V1.2$-VN and $Ca_V1.2$-VC physically interact to form a fluorescent Venus, the channels will likely remain coupled at their C tails for the duration of the experiment.

For these experiments, Venus fluorescence and I_{Ca} were recorded from the same cells before and after the application of a conditioning protocol involving five 500-ms pulses from −80 to +20 mV. $Ca_V1.2$ clusters increased in Venus fluorescence in 2 ways: noninteracting Venus proteins dimerized to create new, fluorescent areas (Fig. 7*B*, ROI 1), or preexisting clusters display additional channel–channel interactions post stimulation (Fig. 7*B*, ROI 2 and 3). Indeed, fluorescence in cells transfected with $Ca_V1.2$-Venus increased by 5% upon stimulation, while $Ca_V1.2$-Venus cotransfected with Kv2.1 increased by 27% (Fig. 7*C*).

Basal (i.e., before preconditioning pulse) I_{Ca} was nearly 3-fold larger in cells coexpressing Kv2.1 and $Ca_V1.2$-VN/VC versus $Ca_V1.2$-VN/VC alone, respectively (Fig. 7*D*). The nonconducting form of Kv2.1, Kv2.1P404W (46), was used for transfection in these experiments so as not to confound any I_{Ca} recordings. The conditioning protocol increased both I_{Ca} and Venus fluorescence to a larger extent in cells coexpressing Kv2.1 and $Ca_V1.2$ than in cells expressing $Ca_V1.2$ alone (Fig. 7*D*). Furthermore, note that membrane depolarization shifted the voltage dependence of G/G_{max} in cells coexpressing $Ca_V1.2$ and Kv2.1 but not in cells transfected with $Ca_V1.2$ only (Fig. 7*E*). These data suggest that coexpression of nonconducting Kv2.1P404W increases the probability of $Ca_V1.2$–$Ca_V1.2$ channel interactions, both at rest and during membrane depolarization. Together, these data support a model that Kv2.1 can enhance $Ca_V1.2$ activity by increasing $Ca_V1.2$ clustering and interaction.

Discussion

Kv2.1 protein is expressed in female and male arterial myocytes, where its assumed functional role has been as a voltage-gated ion channel that, upon opening, hyperpolarizes the membrane potential of these cells to impact myocyte $[Ca^{2+}]_i$ and myogenic tone (16). Here, we propose a model in which Kv2.1 channels have a more complex function to exert opposing actions on vascular smooth muscle. In its canonical role, the opening of conducting Kv2.1 hyperpolarizes arterial myocytes, which decreases the P_o of $Ca_V1.2$ channels. This lowers $[Ca^{2+}]_i$, inducing relaxation. Our data indicate that Kv2.1 protein has an additional nonconducting structural role in arterial myocytes: to enhance $Ca_V1.2$ clustering and activity, thereby increasing $[Ca^{2+}]_i$ and inducing contraction. It is paradoxical that Kv2.1 could control both relaxation and contraction in arterial smooth muscle. Notably, we find that the relative contribution of the electrical and structural roles of Kv2.1 to the control of membrane potential and $Ca_V1.2$ activity, respectively, varies with sex. In male myocytes, the dominant role for Kv2.1 channels is as an ion channel regulating membrane potential. In female myocytes, however, Kv2.1 channels have dual electrical and structural roles in both controlling membrane potential and enhancing $Ca_V1.2$ function, respectively.

Our data suggest that Kv2.1 enhances I_{Ca} by increasing the P_o of $Ca_V1.2$ channels, as the number of $Ca_V1.2$ channels and the amplitude of their unitary currents remain unchanged, regardless of differences in Kv2.1 expression in WT and Kv2.1$^{-/-}$ myocytes. Kv2.1 also shifted the voltage dependence of activation of $Ca_V1.2$ channels toward more hyperpolarized potentials and increased their open times, suggesting that Kv2.1 facilitates $Ca_V1.2$ gating and stabilizes its open conformation. In combination with recently published work (11, 12), the data presented here suggest a potential mechanism by which Kv2.1 acts to increase the P_o of $Ca_V1.2$ channels. We found by PLA that Kv2.1 and $Ca_V1.2$ are in close proximity (i.e., 40 to 60 nm) to one another in arterial myocytes. The increase in $Ca_V1.2$ P_o and open times along with the shift of their voltage dependence of activation are similar to those observed during physical coupling of clustered $Ca_V1.2$ channels (11, 12). Our data support this model in that female myocytes, which have higher Kv2.1 expression, had increased $Ca_V1.2$ cluster area, and coexpression of Kv2.1 increased the probability of interactions of the C tails of clustered $Ca_V1.2$ channels in HEK-293 cells. The exact mechanism by which Kv2.1 organizes $Ca_V1.2$ channels is unclear, but our results support that this may involve an increase in the probability of C tail–C tail interactions, which enhances functional coupling.

Our recent paper describes a potential mechanism by which Kv2.1 could increase $Ca_V1.2$ channel clustering in arterial smooth muscle (8). In these cells, $Ca_V1.2$ cluster formation is determined by a stochastic self-assembly process in which cluster size is determined by 3 distinct biological probabilities: cluster nucleation (P_n), removal (P_R), and growth (P_g). P_n is the first step in cluster formation and is the probability that an ion channel-containing vesicle will be randomly inserted at any site in the membrane. Changes in P_n lead to variations in cluster density. Changes in density as well as cluster size are determined by P_R, the probability of clusters being endocytosed or degraded from the membrane. Lastly, P_g is the probability of a channel being inserted immediately adjacent to preexisting channels. The growth probability of a cluster is P_g multiplied by the number of available neighbors. Thus, an increase in P_g increases cluster area. In Figs. 2 and 6, we show that the level of Kv2.1 expression in female myocytes increased $Ca_V1.2$ channel cluster area, without significant changes in the number of channels in the

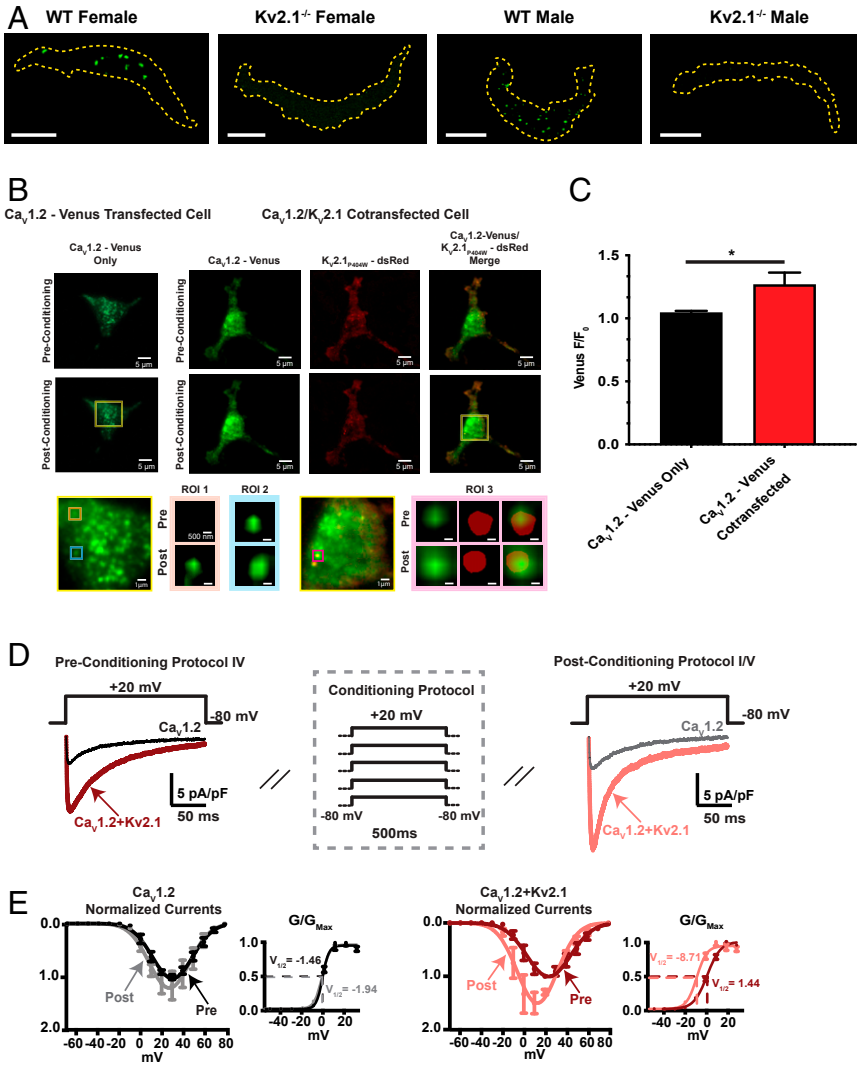

Fig. 7. Kv2.1 channels colocalize with $Ca_V1.2$ channels, promoting $Ca_V1.2$–$Ca_V1.2$ channel interactions. (*A*) PLA images of representative Kv2.1 and $Ca_V1.2$ in WT male and female myocytes. (Scale bars, 15 μm.) (*B*) TIRF images of Venus fluorescence reconstitution in HEK-293 cells expressing $Ca_V1.2$-VN and $Ca_V1.2$-VC or $Ca_V1.2$-VN, $Ca_V1.2$-VC, and $Kv2.1_{P404W}$-dsRed. (*B*, *Insets*) Representative images of dimerization of $Ca_V1.2$-VN and $Ca_V1.2$-VC. ROI, region of interest. (*C*) Bar plot showing the mean Venus fluorescence (F/F_0) ± SEM after depolarization. (*D*) I_{Ca} currents from the HEK-293 cells expressing $Ca_V1.2$-VN and $Ca_V1.2$-VC or $Ca_V1.2$-VN, $Ca_V1.2$-VC, and Kv2.1. (*E*) I–V relationships of mean ± SEM I_{Ca}. G/G_{max} sigmoidal curves clearly show a shift in the activation of $Ca_V1.2$ channels after the protocol, which is more marked in the cells transfected with $Ca_V1.2$-VN, $Ca_V1.2$-VC, and Kv2.1 (~10 mV). *$P < 0.05$.

membrane (i.e., similar P_n) or total $Ca_V1.2$ protein expression. This suggests that Kv2.1 could be acting to increase the P_g of $Ca_V1.2$ channels.

Importantly, loss of Kv2.1 expression decreased but did not eliminate $Ca_V1.2$ channel clusters in arterial myocytes of both sexes. This suggests that Kv2.1 expression is not required for the formation of $Ca_V1.2$ clusters. Indeed, $Ca_V1.2$ cluster size in male WT and $Kv2.1^{-/-}$ myocytes is similar, indicating that the relationship between Kv2.1 expression, $Ca_V1.2$ cluster size, and Ca^{2+} influx is not linear. Thus, a critical number of Kv2.1 channels or ratio of Kv2.1 to $Ca_V1.2$ expression levels could be a key determinant for how Kv2.1 alters $Ca_V1.2$ organization and function. Our Kv2.1 and $Ca_V1.2$ gating current data support this view. We estimated that the total number of $Ca_V1.2$ channels is ~192,000 per arterial myocyte (i.e., ~80 channels per μm^2) regardless of Kv2.1 genotype or sex. However, the number of Kv2.1 channels varies in a sex-specific manner. Female and male myocytes express ~183,000 (~76 channels per μm^2) and 75,000 channels (~31 channels per μm^2), respectively. Thus, the ratio of Kv2.1:$Ca_V1.2$ channels is ~1:1 in female versus 0.4:1 in male mesenteric myocytes. That the size of $Ca_V1.2$ clusters and the amplitude of I_{Ca} were similar in male WT and $Kv2.1^{-/-}$ myocytes suggests that this 0.4:1 expression ratio is not sufficient to alter $Ca_V1.2$ organization and function. We note that this nonlinearity could also suggest that, in addition to Kv2.1 expression levels, other factors might contribute to the observed sex-specific differences in $Ca_V1.2$ function. Future studies should investigate whether the ~1:1 Kv2.1:$Ca_V1.2$ channel ratio observed in female myocytes is the lower limit or optimal point for the modulation of $Ca_V1.2$ cluster size and channel–channel interactions, and any additional mechanisms that may act in concert with Kv2.1 expression level to impact $Ca_V1.2$ function.

An intriguing finding in this study is that, as in heterologous expression systems (20–22), the vast majority of Kv2.1 channels in male and female arterial myocytes are nonconductive. One potential hypothesis is that conductive and nonconductive Kv2.1 channels have separate functional roles, with conductive channels regulating membrane potential and nonconductive channels

acting to increase the P_g and P_o of clustered $Ca_V1.2$ channels. Several observations are consistent with this hypothesis. First, our data suggest that Kv2.1 and $Ca_V1.2$ colocalize. Second, we show that at sites where Kv2.1 and $Ca_V1.2$ channels cocluster, $Ca_V1.2$–$Ca_V1.2$ interactions take place. Third, it has been proposed that the bulk of clustered Kv2.1 channels may be in a nonconductive state (21). These observations suggest the hypothesis that nonconductive Kv2.1 channels are involved in the clustering and activity of $Ca_V1.2$ channels.

While the evidence for nonconductive Kv2.1 channels playing a role in $Ca_V1.2$ clustering is strong, our data do not allow us to determine if the sole function of clustered Kv2.1 is to bring $Ca_V1.2$ channels together. However, our recent paper (30) as well as other work from the Trimmer (46, 47) and Tamkun (48) laboratories support that clustered Kv2.1 channels are involved in the formation of endoplasmic reticulum–plasma membrane junctions in HEK-293 cells and hippocampal neurons. In hippocampal neurons, Kv2.1-expressing endoplasmic reticulum–plasma membrane junctions contain functional ryanodine receptors that produce Ca^{2+} sparks both at rest and during membrane depolarization (30). Whether this same phenomenon happens in arterial smooth muscle cells is currently unknown. Future experiments should investigate whether Kv2.1 promotes the formation of sarcoplasmic reticulum–sarcolemmal junctions in arterial myocytes as it does in HEK-293 cells and hippocampal neurons. Further studies should consider if, in arterial myocytes, these Kv2.1-containing junctions form in combination with junctophilin-2 (49), and whether due to their differing levels of Kv2.1 expression these structures are more prominent in female than in male myocytes.

An additional question raised by this study is the nature of the mechanisms underlying the differential expression of Kv2.1 channels in male and female arterial myocytes. To our knowledge, there are no published studies addressing whether the expression of Kv2.1 or Kv9.3 in smooth muscle is regulated by sex hormones. Interestingly, Vierra et al. (30) did not detect sex-specific differences in Kv2.1 expression or $Ca_V1.2$ clustering and function in hippocampal neurons. However, others have suggested that estrogen down-regulates Kv1.5 but has no effect on Kv2.1 expression in female mouse ventricular myocytes (50). Interestingly, we find that Kv1.5 expression is similar in male and female arterial myocytes. Thus, the control of expression of these proteins by sex hormones is complex and likely varies among cell types. A follow-up study should investigate the role of sex hormones in the regulation of Kv2.1 in arterial myocytes.

The experiments in this study were performed using a global constitutive Kv2.1 knockout mouse. Therefore, we cannot rule out the possibility of long-term and systemic compensatory mechanisms impacting arterial function. That said, in Vierra et al. (30), we reported that coexpression of WT Kv2.1 and $Ca_V1.2$ channels enhances $Ca_V1.2$ clustering in HEK-293 cells and hippocampal neurons. Expression of a Kv2.1 channel that does not cluster, $Kv2.1_{S586A}$, failed to promote $Ca_V1.2$ clustering. Furthermore, we showed that in HEK-293 cells and hippocampal neurons, $Ca_V1.2$ clustering appears to be rapidly and dynamically regulated by treatments that impact Kv2.1 clustering. These data suggest that $Ca_V1.2$ clustering is directly and actively controlled by the level of expression and clustering state of Kv2.1 channels and that the sex-specific differences we observed are smooth muscle specific.

To conclude, we propose that Kv2.1 channels have dual conducting and structural roles with opposing functional consequences in arterial smooth muscle. Conductive Kv2.1 channels oppose vasoconstriction by inducing membrane hyperpolarization. Paradoxically, by promoting the structural clustering of the $Ca_V1.2$ channel, Kv2.1 enhances Ca^{2+} influx and induces vasoconstriction. Sex-specific differences in Kv2.1 expression as well as the nonlinear relationship between Kv2.1 expression, clustering, and activity shift the balance between the hyperpolarizing and Ca^{2+} entry actions of Kv2.1. These consequences ultimately lead to differences in the regulation of membrane potential, intracellular Ca^{2+}, and myogenic tone between male and female arteries.

Materials and Methods

A detailed version of this study's materials and methods can be found in *SI Appendix*. Briefly, male and female WT C57BL/6J and $Kv2.1^{-/-}$ mice were used in this study. Experiments were conducted within Institutional Animal Care and Use Committee guidelines. Electrophysiological recording techniques were performed using Axopatch amplifiers. Protein levels were determined using immunoblot approaches. $[Ca^{2+}]_i$ imaging was performed using an Andor Diskovery spinning disk system. Immunofluorescence TIRF, superresolution, and confocal images were acquired using a Leica GSD or Olympus FV3000 microscope.

Data Availability Statement. All data are available in the manuscript and *SI Appendix*.

ACKNOWLEDGMENTS. We thank Dellaney Rudolph-Gandy for technical assistance. Thanks also to Dr. Manuel F. Navedo for help with the analysis of data. Guangxitoxin-1E, kindly provided by Dr. Jon Sack, was synthesized at the Molecular Foundry of the Lawrence Berkeley National Laboratory under US Department of Energy Contract DE-AC02-05CH11231. The study was supported by grants from the US NIH (5R01HL085686, 1R01HL144071, 1OT2OD026580, T32HL086350) and American Heart Association (18PRE33960249).

1. W. M. Bayliss, On the local reactions of the arterial wall to changes of internal pressure. *J. Physiol.* **28**, 220–231 (1902).
2. A. L. Gonzales *et al.*, A PLCγ1-dependent, force-sensitive signaling network in the myogenic constriction of cerebral arteries. *Sci. Signal.* **7**, ra49 (2014).
3. M. A. Spassova, T. Hewavitharana, W. Xu, J. Soboloff, D. L. Gill, A common mechanism underlies stretch activation and receptor activation of TRPC6 channels. *Proc. Natl. Acad. Sci. U.S.A.* **103**, 16586–16591 (2006).
4. S. Bulley *et al.*, Arterial smooth muscle cell PKD2 (TRPP1) channels regulate systemic blood pressure. *eLife* **7**, e42628 (2018).
5. M. F. Navedo, L. F. Santana, $Ca_V1.2$ sparklets in heart and vascular smooth muscle. *J. Mol. Cell. Cardiol.* **58**, 67–76 (2013).
6. M. F. Navedo, G. C. Amberg, V. S. Votaw, L. F. Santana, Constitutively active L-type Ca^{2+} channels. *Proc. Natl. Acad. Sci. U.S.A.* **102**, 11112–11117 (2005).
7. G. C. Amberg, M. F. Navedo, M. Nieves-Cintrón, J. D. Molkentin, L. F. Santana, Calcium sparklets regulate local and global calcium in murine arterial smooth muscle. *J. Physiol.* **579**, 187–201 (2007).
8. D. Sato *et al.*, A stochastic model of ion channel cluster formation in the plasma membrane. *J. Gen. Physiol.* **151**, 1116–1134 (2019).
9. M. F. Navedo *et al.*, Increased coupled gating of L-type Ca^{2+} channels during hypertension and Timothy syndrome. *Circ. Res.* **106**, 748–756 (2010).
10. E. P. Cheng *et al.*, Restoration of normal L-type Ca^{2+} channel function during Timothy syndrome by ablation of an anchoring protein. *Circ. Res.* **109**, 255–261 (2011).
11. R. E. Dixon, C. Yuan, E. P. Cheng, M. F. Navedo, L. F. Santana, Ca^{2+} signaling amplification by oligomerization of L-type $Ca_v1.2$ channels. *Proc. Natl. Acad. Sci. U.S.A.* **109**, 1749–1754 (2012).
12. R. E. Dixon *et al.*, Graded Ca^{2+}/calmodulin-dependent coupling of voltage-gated $Ca_V1.2$ channels. *eLife* **4**, e05608 (2015).
13. M. T. Nelson *et al.*, Relaxation of arterial smooth muscle by calcium sparks. *Science* **270**, 633–637 (1995).
14. G. C. Amberg, L. F. Santana, Kv2 channels oppose myogenic constriction of rat cerebral arteries. *Am. J. Physiol. Cell Physiol.* **291**, C348–C356 (2006).
15. F. Plane *et al.*, Heteromultimeric Kv1 channels contribute to myogenic control of arterial diameter. *Circ. Res.* **96**, 216–224 (2005).
16. X. Z. Zhong *et al.*, Stromatoxin-sensitive, heteromultimeric Kv2.1/Kv9.3 channels contribute to myogenic control of cerebral arterial diameter. *J. Physiol.* **588**, 4519–4537 (2010).
17. S. L. Archer *et al.*, Molecular identification of the role of voltage-gated K^+ channels, Kv1.5 and Kv2.1, in hypoxic pulmonary vasoconstriction and control of resting membrane potential in rat pulmonary artery myocytes. *J. Clin. Invest.* **101**, 2319–2330 (1998).
18. Y. Lu, S. T. Hanna, G. Tang, R. Wang, Contributions of Kv1.2, Kv1.5 and Kv2.1 subunits to the native delayed rectifier K(+) current in rat mesenteric artery smooth muscle cells. *Life Sci.* **71**, 1465–1473 (2002).
19. G. C. Amberg, C. F. Rossow, M. F. Navedo, L. F. Santana, NFATc3 regulates Kv2.1 expression in arterial smooth muscle. *J. Biol. Chem.* **279**, 47326–47334 (2004).
20. K. Benndorf, R. Koopmann, C. Lorra, O. Pongs, Gating and conductance properties of a human delayed rectifier K^+ channel expressed in frog oocytes. *J. Physiol.* **477**, 1–14 (1994).
21. K. M. O'Connell, R. Loftus, M. M. Tamkun, Localization-dependent activity of the Kv2.1 delayed-rectifier K^+ channel. *Proc. Natl. Acad. Sci. U.S.A.* **107**, 12351–12356 (2010).

22. P. D. Fox, R. J. Loftus, M. M. Tamkun, Regulation of Kv2.1 K(+) conductance by cell surface channel density. *J. Neurosci.* **33**, 1259–1270 (2013).
23. J. S. Trimmer, Immunological identification and characterization of a delayed rectifier K^+ channel polypeptide in rat brain. *Proc. Natl. Acad. Sci. U.S.A.* **88**, 10764–10768 (1991).
24. D. E. Antonucci, S. T. Lim, S. Vassanelli, J. S. Trimmer, Dynamic localization and clustering of dendritic Kv2.1 voltage-dependent potassium channels in developing hippocampal neurons. *Neuroscience* **108**, 69–81 (2001).
25. R. H. Scannevin, H. Murakoshi, K. J. Rhodes, J. S. Trimmer, Identification of a cytoplasmic domain important in the polarized expression and clustering of the Kv2.1 K^+ channel. *J. Cell Biol.* **135**, 1619–1632 (1996).
26. S. T. Lim, D. E. Antonucci, R. H. Scannevin, J. S. Trimmer, A novel targeting signal for proximal clustering of the Kv2.1 K^+ channel in hippocampal neurons. *Neuron* **25**, 385–397 (2000).
27. D. P. Mohapatra, J. S. Trimmer, The Kv2.1 C terminus can autonomously transfer Kv2.1-like phosphorylation-dependent localization, voltage-dependent gating, and muscarinic modulation to diverse Kv channels. *J. Neurosci.* **26**, 685–695 (2006).
28. M. M. Cobb, D. C. Austin, J. T. Sack, J. S. Trimmer, Cell cycle-dependent changes in localization and phosphorylation of the plasma membrane Kv2.1 K^+ channel impact endoplasmic reticulum membrane contact sites in COS-1 cells. *J. Biol. Chem.* **290**, 29189–29201 (2015).
29. P. D. Fox *et al*., Induction of stable ER-plasma-membrane junctions by Kv2.1 potassium channels. *J. Cell Sci.* **128**, 2096–2105 (2015).
30. N. C. Vierra, M. Kirmiz, D. van der List, L. F. Santana, J. S. Trimmer, Kv2.1 mediates spatial and functional coupling of L-type calcium channels and ryanodine receptors in mammalian neurons. *eLife* **8**, e49953 (2019).
31. J. Gayet-Primo, D. B. Yaeger, R. A. Khanjian, T. Puthussery, Heteromeric $K_V2/K_V8.2$ channels mediate delayed rectifier potassium currents in primate photoreceptors. *J. Neurosci.* **38**, 3414–3427 (2018).
32. D. C. Tilley *et al*., The tarantula toxin GxTx detains K^+ channel gating charges in their resting conformation. *J. Gen. Physiol.* **151**, 292–315 (2019).
33. M. Taglialatela, E. Stefani, Gating currents of the cloned delayed-rectifier K^+ channel DRK1. *Proc. Natl. Acad. Sci. U.S.A.* **90**, 4758–4762 (1993).
34. A. Scholle *et al*., Effects of Kv1.2 intracellular regions on activation of Kv2.1 channels. *Biophys. J.* **87**, 873–882 (2004).
35. A. Jara-Oseguera *et al*., Uncoupling charge movement from channel opening in voltage-gated potassium channels by ruthenium complexes. *J. Biol. Chem.* **286**, 16414–16425 (2011).
36. E. Bocksteins, A. J. Labro, D. J. Snyders, D. P. Mohapatra, The electrically silent Kv6.4 subunit confers hyperpolarized gating charge movement in Kv2.1/Kv6.4 heterotetrameric channels. *PLoS One* **7**, e37143 (2012).
37. A. J. Patel, M. Lazdunski, E. Honoré, Kv2.1/Kv9.3, a novel ATP-dependent delayed-rectifier K^+ channel in oxygen-sensitive pulmonary artery myocytes. *EMBO J.* **16**, 6615–6625 (1997).
38. R. H. Cox, S. Fromme, Functional expression profile of voltage-gated K(+) channel subunits in rat small mesenteric arteries. *Cell Biochem. Biophys.* **74**, 263–276 (2016).
39. C. M. Armstrong, F. Bezanilla, Currents related to movement of the gating particles of the sodium channels. *Nature* **242**, 459–461 (1973).
40. L. D. Islas, F. J. Sigworth, Voltage sensitivity and gating charge in Shaker and Shab family potassium channels. *J. Gen. Physiol.* **114**, 723–742 (1999).
41. R. W. Hadley, W. J. Lederer, Properties of L-type calcium channel gating current in isolated guinea pig ventricular myocytes. *J. Gen. Physiol.* **98**, 265–285 (1991).
42. F. Noceti *et al*., Effective gating charges per channel in voltage-dependent K^+ and Ca^{2+} channels. *J. Gen. Physiol.* **108**, 143–155 (1996).
43. D. W. Ito *et al*., β-adrenergic-mediated dynamic augmentation of sarcolemmal Ca_V 1.2 clustering and co-operativity in ventricular myocytes. *J. Physiol.* **597**, 2139–2162 (2019).
44. Y. Kodama, C. D. Hu, An improved bimolecular fluorescence complementation assay with a high signal-to-noise ratio. *Biotechniques* **49**, 793–805 (2010).
45. C. M. Moreno *et al*., Ca(2+) entry into neurons is facilitated by cooperative gating of clustered $Ca_V1.3$ channels. *eLife* **5**, e15744 (2016).
46. M. Kirmiz *et al*., Remodeling neuronal ER-PM junctions is a conserved nonconducting function of Kv2 plasma membrane ion channels. *Mol. Biol. Cell* **29**, 2410–2432 (2018).
47. M. Kirmiz, N. C. Vierra, S. Palacio, J. S. Trimmer, Identification of VAPA and VAPB as Kv2 channel-interacting proteins defining endoplasmic reticulum-plasma membrane junctions in mammalian brain neurons. *J. Neurosci.* **38**, 7562–7584 (2018).
48. B. Johnson *et al*., Kv2 potassium channels form endoplasmic reticulum/plasma membrane junctions via interaction with VAPA and VAPB. *Proc. Natl. Acad. Sci. U.S.A.* **115**, E7331–E7340 (2018).
49. H. A. T. Pritchard *et al*., Nanoscale coupling of junctophilin-2 and ryanodine receptors regulates vascular smooth muscle cell contractility. *Proc. Natl. Acad. Sci. U.S.A.* **116**, 21874–21881 (2019).
50. T. Saito *et al*., Estrogen contributes to gender differences in mouse ventricular repolarization. *Circ. Res.* **105**, 343–352 (2009).